

Magnetic Interaction in Doped 2D Perovskite Cuprates with Nanoscale Inhomogeneity: Lattice Nonlocal Effects vs Superexchange

Vladimir A. Gavrichkov* and Semyon I. Polukeev

Kirensky Institute of Physics, Akademgorodok 50, bld.38, Krasnoyarsk, 660036 Russia

(Dated: May 25, 2022)

We have studied the superexchange interaction J_{ij} in doped 2D cuprates. The AFM interaction strongly depends on the state of the lattice of CuO_2 layer surrounded by two LaO rock salt layers. In a static U and D stripe nanostructure, the homogeneous AFM interaction is impossible due to the U/D periodic stripe sequence and $T_N = 0$. In a dynamic stripe nanostructure, the ideal CuO_2 layer with nonlocal effects and the homogeneous AFM interaction are restored. However the interaction J_{ij} decreases by the exponential factor due to partial dynamical quenching. The meaning of the transition from the dynamic to the static cases lies in spontaneous symmetry θ -breaking with respect to a rotation of the tilted all CuO_6 octahedra by an orientation angle $\delta\theta = n \cdot (45^\circ)$ in the U and D stripe nanostructure of CuO_2 layer.

I. INTRODUCTION

The unique functionality of several materials with perovskite structure, like cuprates,^{1–4} can be tuned by atomic substitutions, tolerance factor, misfit strain and pressure which control structural tilts and nanoscale phase separation.

The scanning tunneling microscopy and spectroscopy (STM and STS)^{5–9} and advanced experimental X-ray methods^{10–14} in a wide range of temperature and doping unambiguously indicate there is a clear connection between the multiscale stripe texture and the quantum coherence of quasiparticles in 2D perovskite high-T_c superconductors. The stripe charge nanostructure is also accompanied by spin inhomogeneity^{15–22}, and the high-temperature superconductivity (HTSC) is believed to originate from magnetic spin excitations that bind Cooper pairs^{23–26}. A magnetic interaction in parent *AFM* 2D cuprates is well known superexchange interaction.²⁷ The *AFM* interaction between the nearest spins of Cu^{2+} ions in the CuO_2 layer is strong ($\sim 0.146\text{eV}$)²⁸ and is much stronger than the interplanar exchange, that mainly responsible for the long range magnetic ordering observed in the nondoped cuprates. For La_2CuO_4 (LCO), the Neel temperature is $T_N \approx 300\text{K}$. In the traditional picture of BCS superconductivity, magnetism destroys Cooper pairs. However, superconductivity in these HTSCs develops from a “bad metal”, whose resistivity is higher than that of BCS superconductors, and the *AFM* magnetism itself is related to the initial “bad metal” state, where superconductivity occurs when long-range magnetic ordering is suppressed at a relatively weak hole doping ($x \sim 0.01$). Indeed, in the resonating-valence bond (RVB) approach and the $t-J$ model,^{23,29–32} the HTSC emerges due to the condensation of hole pairs, induced by the exchange interaction J_{ij} . Pairing of holes in this mechanism is caused by interband quasiparticles transfer in the CuO_2 layer with a short-range *AFM* ordering. Retardation effects for this mechanism are insignificant. Another view on HTSC state in the cuprates (see for example^{33,34}) has been that *AFM* spin fluc-

tuations, becoming particularly longer ranged and soft at low hole doping. In fact, there is the resonant magnetic mode^{35–37} within the *HTSC* phase, where the spin fluctuations scenario represent the lowest bosonic mode relevant for the d-wave *HTSC* pairing in an energy range $\sim J_{ij}$.

If the interaction J_{ij} is a reliable candidate for glue for holes, then how will it change in the inhomogeneity nanostructure of doped 2D cuprates? Here we have studied a specific stripe mechanism that establishes the relationship between the observed nanoscale inhomogeneity and the superexchange J_{ij} . Furthermore, this is a good reason to test your feelings in accordance with the opinion: “...there remains the nagging feeling that even if the basic pairing mechanism ultimately arises from the short-range antiferromagnetic correlations in the layer, some important ingredient may be missing from the theory we have described.” (see the review²⁴).

II. COLOR APPROACH TO NANOSCALE INHOMOGENEITY AND D AND U STRIPE STRUCTURE

The idea of the color approach³⁸ is stripe identification due to the tilting effects (tilting CuO_6 octahedron as a whole).³⁹ The fact is that different stripes differ not only in the hole concentration and spin, but in the type of nuclear configuration (see Fig.1) We have classified the observed stripe configurations into a ninth-order symmetric Abelian group $G(\alpha)$ consisting of two types of stripes $U(\theta_U)$ and $D(\theta_D)$ rotated at right angle relative to each other.³⁸ The sought stripe group $G(\alpha)$ represents all possible reaction products between different initial nuclear configurations in the form of group multiplication, where an ideal nontilted prototype of a perovskite CuO_6 octahedron used as the group unit. In all “structural reactions” of nuclear configurations of stripes, the tilting angle α of the perovskite octahedron with respect to the rock salt LaO layers is saved, but not their initial symmetry, as is the case, for example, in chemical reactions, in accordance with the Woodworth-

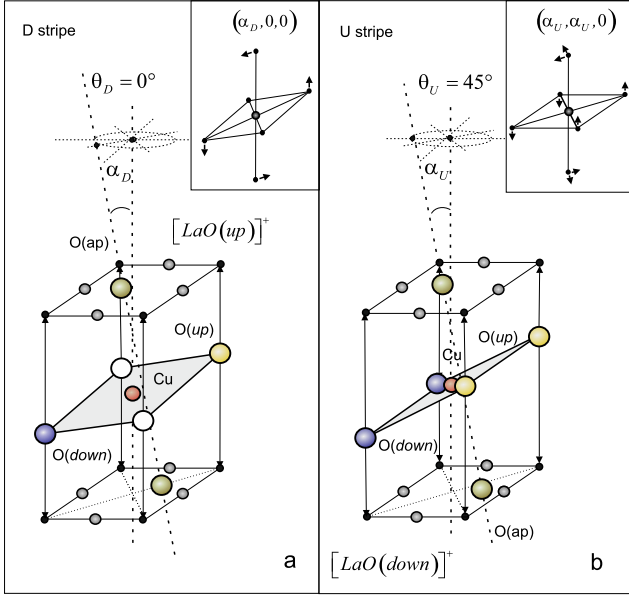


FIG. 1. View of the tilted CuO_6 octahedra of the D (a) and U (b) stripes with different tilting effects in $LSCO$. Insets show the tilting effects in accordance with Glazer's notations.⁴⁰

Hoffman rules.⁴¹ The number of nuclear configurations of the observed stripes in $LSCO$, is reduced to one of the two $U(\theta_U)$ (where $\theta_U = 45^\circ, 135^\circ, 225^\circ, 315^\circ$) or $D(\theta_D)$ (where $\theta_D = 0, 90^\circ, 180^\circ, 270^\circ$) stripes, and their spatial distribution in CuO_2 layer is represented by possible plane graphs with chromatic number $\chi \leq 4$ in the four-color theorem. In four colors, $U(45^\circ), U(225^\circ)$ - red (R), $U(135^\circ), U(315^\circ)$ - blue (B) and also $D(0^\circ), D(180^\circ)$ - green (G); $D(90^\circ), D(270^\circ)$ - yellow (Y), we can always color an arbitrary plane map, and the four colors R, G, B, Y are just four subgroups in $G(\alpha)$. The group can also be represented as a direct product of subgroups of any different colors, e.g. $G(\alpha) = R \times B = G \times Y$ and so on. $D(\theta_D)$ stripes occur as overlapping different $U(\theta_U)$ and $U(\theta_U \pm 90^\circ)$ stripes in an $R/G/B$ sequence, for example, when disordering $U(\theta_U)$ stripes with doping, and vice versa, $U(\theta_U)$ stripes can occur as the overlapping $D(\theta_D)$ and $D(\theta_D \pm 90^\circ)$ stripes in a $G/R/Y$ sequence. These two stripe sequences can be combined into one, for example into $Y/R/G/B$, from which, by rotating all tilted CuO_6 octahedra around from the c axis by the angle $\delta\theta = n \cdot (45^\circ)$, we can obtain three more $B/Y/R/G$, $G/B/Y/R$ and $R/G/B/Y$. The rotation also leads to an shift over $G(\alpha)$ group and transverse shift of linear stripe and diagonal shift of checkerboard structures in Fig.2a,b. This means that the ground state of the CuO_2 layer in Figs.2,3 is fourfold degenerate with respect to the rotation. Indeed, we can also form a novel JT cell (see Fig.3), during the translation of which the number of hole carriers and spins in the JT cell are saved. The state Ψ_{θ_n} of the JT cell is fourfold degenerate by the initial phase $\theta_n = 0, 45^\circ, 90^\circ, 135^\circ$, which splits at tunneling CuO_6 octahedra over states of the $D(\theta_D)$ and $U(\theta_U)$

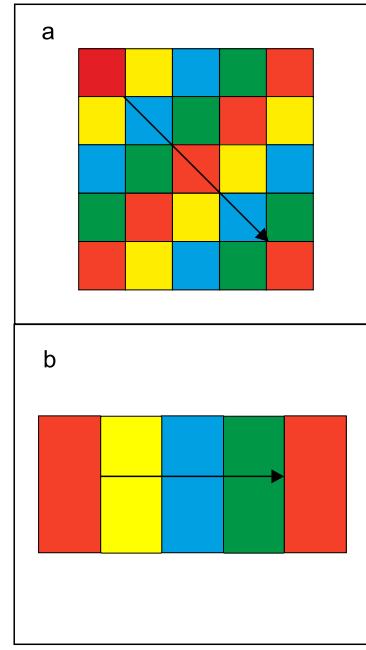


FIG. 2. Regular checkerboard (a) and linear (b) stripe structures corresponding to the chromatic number $\chi = 2$. The arrows show the shift of the stripe structure when all CuO_6 octahedra are rotated by the angle $\delta\theta = 45^\circ$. The stripe structure are also shown in Fig.3 in more detail.

stripes. In particular, if the D and U stripe widths are equal, any CuO_6 octahedron can be located simultaneously both in D , and U stripes without a certain the angle θ , and ideal CuO_2 layer structure being restored. At the spontaneous θ -symmetry breaking, a static picture that is formed with the help of JT cell is shown in Fig.3, where the latter contains more than a dozen CuO_6 octahedra, i.e. the four octahedra on the single stripe.

Let us consider the JT cell to understand a nature of inhomogeneous distribution of hole and spin density in the CuO_2 layer. The cell has a Jahn-Teller (JT) nature, shown in Fig.4, where the (pseudo) JT effect is non-local, and is associated with the presence of positive charged LaO rock salt layers. The tilting angle α_U at the orientation angle θ_U corresponds to relaxation a_{1g} modes, and the tilting angle α_D at the orientation angle θ_D corresponds to JT active b_{1g} modes.

The absence of the superconductivity in the AFM CuO layers on graphene^{42,43} points to a key role of rock salt LaO layers in 2D doped cuprates.⁴ The direct similarity of the structures of the nondoped LCO and the non- JT La_2NiO_4 materials,⁴⁴ where ions Ni^{2+} is in the high spin state $S = 1$, also points to missing JT effect in the $N_0(d^9)$ sector of the configuration space of CuO_2 layer. However, in the $N_-(d^8)$ sector of doped $LSCO$ the hole carriers are at the Zhang-Rice singlet state $^1A_{1g}$,⁴⁵ and it's a JT state.⁴⁶ Moreover, JT effect depends on the doping concentration in a threshold way. Indeed the hole carriers in $D(\theta_D)$ stripes can induce a non-local JT

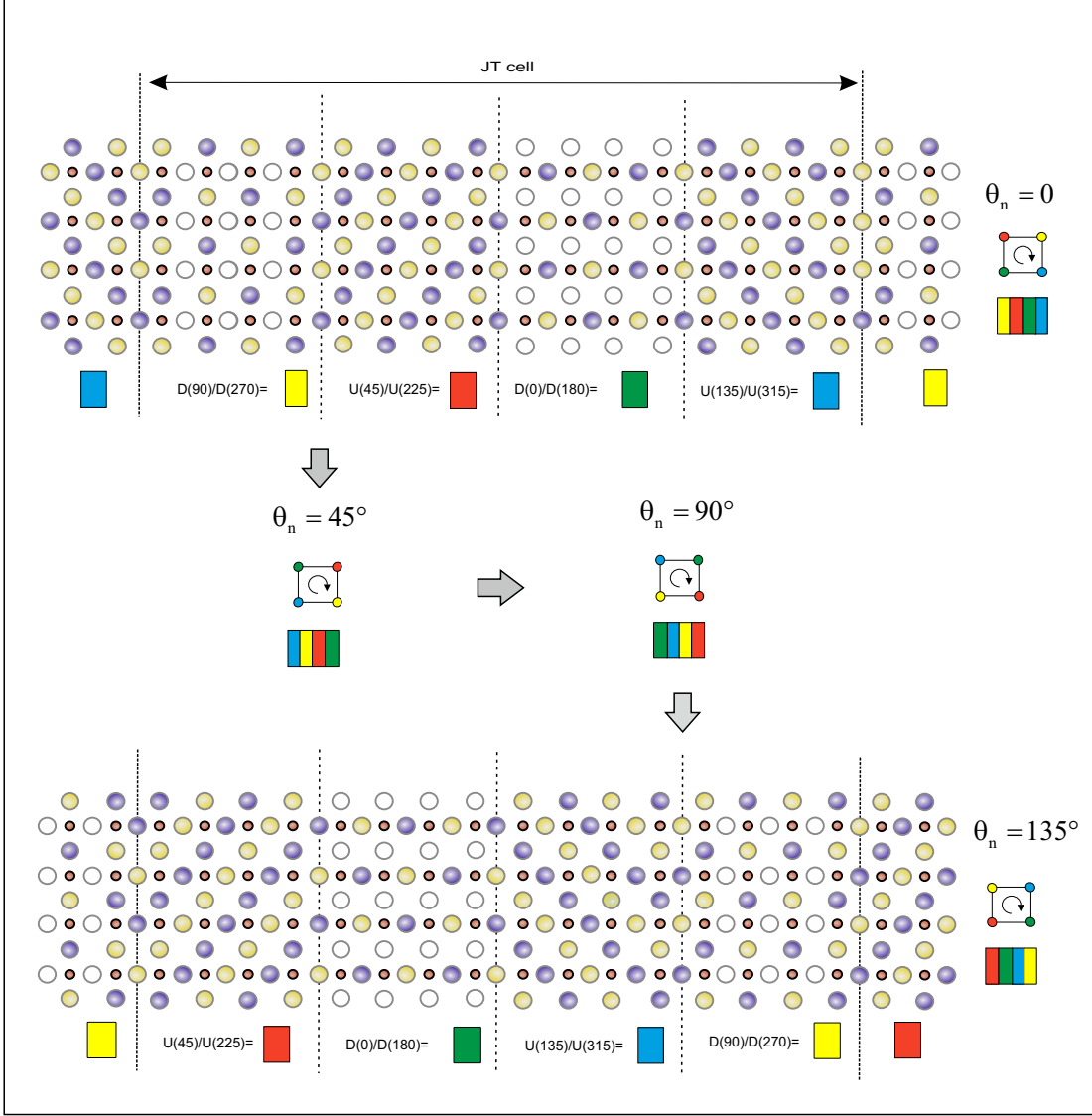


FIG. 3. Structural motive for the fourfold degenerate state Ψ_{θ_n} of the novel JT cell. On the right is the initial phase θ_n , Ψ_{θ_n} - color code and coloring of the graph with $\chi = 2$.

(pseudo-)effect with a hamiltonian (see Fig.4a,b)

$$\hat{H}_{JT}(Q_\alpha, Q_\theta) = \varepsilon_{^1B_{1g}} \sum_{\sigma} b_{i\sigma}^+ b_{i\sigma} + \varepsilon_{^1A_{1g}} \sum_{\sigma} a_{i\sigma}^+ a_{i\sigma} + V_{b_{1g}} Q_\alpha \sum_{\sigma} (a_{i\sigma}^+ b_{i\sigma} + b_{i\sigma}^+ a_{i\sigma}) + U(Q_\alpha, Q_\theta) \quad (1)$$

in the hole sector $N_-(d^8)$ of the configuration space of the CuO_2 layer (see Fig.4). Here is $a_{i\sigma}^+ = \eta(\sigma) X_i^{^1B_{1g}, \bar{\sigma}_b}$ and $b_{i\sigma}^+ = \eta(\sigma) X_i^{^1A_{1g}, \bar{\sigma}_b}$ are two hole parts of the quasi-

particle operator

$$\begin{aligned} d_{i\lambda\sigma}^+ &= X_i^{\sigma_b, A_{1g}} + \sum_{h=^1A_g, ^1B_g} \langle h | d_{i\lambda\sigma}^+ | \sigma_b \rangle X_i^{h, \bar{\sigma}_b} = (2) \\ &= X_i^{\sigma_b, A_{1g}} + \begin{cases} a_{i\sigma}^+, \lambda = 3z^2 - r^2 \\ b_{i\sigma}^+, \lambda = x^2 - y^2 \end{cases} \end{aligned}$$

generating the two-hole $^1A_{1g}$ and $^1B_{1g}$ states in the $N_-(d^8)$ sector. If $|h\rangle = |^1A_{1g}\rangle$, then the operator $d_{i\lambda\sigma}^+$

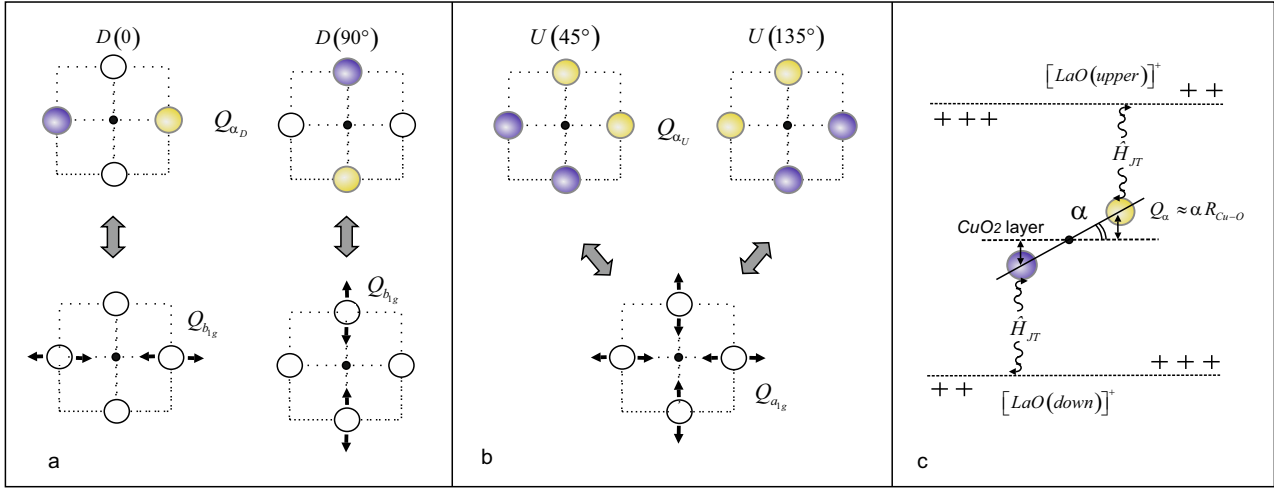


FIG. 4. Graphic scheme: (a) b_{1g} tilting modes active in the non-local CuO_6 octahedron JT effect, as well as (b) a_{1g} relaxation modes in D and U stripes. Arrows in (a) and (b) show the relationship between tilting and conventional local modes. (c) Non-local JT effect in CuO_2 layer surrounded by the symmetrical LaO rock salt layers.

takes the well-known form for the Hubbard model.⁴⁷ It is assumed the $U(Q_\alpha, Q_\theta)$ potential is created by the LaO rock salt layers, and the equilibrium ion positions in CuO_2 layer can be obtained from the equation $\frac{\partial \hat{H}_{JT}(Q_\alpha, Q_\theta)}{\partial Q_\alpha \partial Q_\theta} = 0$. Here we just use the set θ_D and $\alpha_D \approx 14^\circ \div 18^\circ$, which are observed at $T = 100K$ for D stripes.³⁹ The hole concentration dependence of the magnitude $\alpha_D(x)$ in the JT effect can be obtained using u/v transformation in the hamiltonian (1) with coefficients

$$u^2(Q_\alpha) = \frac{1}{2} \left(1 - \frac{\varepsilon_{A_{1g}} - \varepsilon_{B_{1g}}}{D(Q_\alpha)} \right), \quad (3)$$

$$v^2(Q_\alpha) = \frac{1}{2} \left(1 + \frac{\varepsilon_{A_{1g}} - \varepsilon_{B_{1g}}}{D(Q_\alpha)} \right),$$

where $D(Q_\alpha) = \sqrt{(\varepsilon_{A_{1g}} - \varepsilon_{B_{1g}})^2 + 4(IQ_\alpha)^2}$ and $a_{i\sigma}^+ = v(Q_\alpha) \tilde{a}_{i\sigma}^+ + u(Q_\alpha) \tilde{b}_{i\sigma}^+$, $b_{i\sigma}^+ = u(Q_\alpha) \tilde{a}_{i\sigma}^+ - v(Q_\alpha) \tilde{b}_{i\sigma}^+$. Then hamiltonian (1) may be written

$$\hat{H}_{JT}(Q_\alpha, Q_{\theta_D}) = \varepsilon_+(Q_\alpha) \sum_{\sigma} \tilde{b}_{i\sigma}^+ \tilde{b}_{i\sigma} + \varepsilon_-(Q_\alpha) \sum_{\sigma} \tilde{a}_{i\sigma}^+ \tilde{a}_{i\sigma}, \quad (4)$$

where $\varepsilon_{\pm}(Q_\alpha) = \frac{1}{2} [\varepsilon_{A_{1g}} + \varepsilon_{B_{1g}} \pm D(Q_\alpha)]$ are the energies of hole quasiparticles in two-hole singlets $|^1\tilde{A}_{1g}\rangle$ and $|^1\tilde{B}_{1g}\rangle$ taking into account the JT interaction $V_{b_{1g}}$.

The equilibrium tilting angle α_D is obtained from the condition $\frac{\partial \hat{H}_{JT}(Q_\alpha, Q_{\theta_D})}{\partial \alpha} = 0$ for the minimum adiabatic potential $\varepsilon_{\pm}(Q_\alpha)$. One at $U(Q_\alpha, Q_{\theta_D}) \approx (k_\alpha \alpha^2)/2$ take the form $\alpha_D = \pm \sqrt{\left(\frac{R_D V_{b_{1g}}}{k_{\alpha_D}}\right)^2 - \left(\frac{\Delta}{V_{b_{1g}}}\right)^2}$ where $R_D = \sum_{\sigma} \langle \tilde{b}_{\sigma}^+ \tilde{b}_{\sigma} - \tilde{a}_{\sigma}^+ \tilde{a}_{\sigma} \rangle$. Thus, in doped LSCO cuprates there is a hole doping level $x_c = \langle X_i^{^1\tilde{A}_{1g}} X_i^{^1\tilde{A}_{1g}} - X_i^{^1\tilde{B}_{1g}} X_i^{^1\tilde{B}_{1g}} \rangle$ =

$\frac{k_\alpha \Delta}{2V_{b_{1g}}^2}$, above which in D stripes, a JT pseudo effect with $\alpha_D \neq 0$ can be observed. At $\Delta = \varepsilon_{A_{1g}} - \varepsilon_{B_{1g}} = 0$ ⁴⁸ we obtain the quadratic concentration dependence of the JT contribution:

$$\hat{H}_{JT}(Q_{\alpha_D}, Q_{\theta_D}) = -E_{JT} R \sum_{\sigma} \left(\tilde{b}_{i\sigma}^+ \tilde{b}_{i\sigma} - \tilde{a}_{i\sigma}^+ \tilde{a}_{i\sigma} \right), \quad (5)$$

where $E_{JT} = V_{b_{1g}}^2 / 2k_\alpha$. Any homogeneous hole density at $x < x_c$ will be unstable to creating the local D areas with a higher hole density $x_D > x_c$. Without a dependence of elasticity value $k_\alpha(x)$, a minimum of the adiabatic potential corresponds to the hole concentration $x = 1$.

III. ELECTRON-HOLE PAIRS IN SUPEREXCHANGE INTERACTION

3.1 Let's consider the superexchange interaction J_{ij} in a static stripe structure in Fig.3. In the case of spontaneous θ -symmetry breaking (the JT cell state Ψ_{θ_n} is nondegenerate), the doped LSCO cuprate has a static nanostructure, where the exchange interaction are missing in the D stripes, and in the U stripes the superexchange interaction is equal to the one in nondoped LCO material:

$$\hat{H}_S = - \sum_{ij} J_{ij}^{tot} \hat{S}_i \hat{S}_j \quad (6)$$

where the interaction $J_{ij}^{tot} = \sum_{h,e} J_{ij}(h,e)$ can be calculated in the adiabatic approximation. Superexchange interaction (6) arises as a result of the superposition of contributions from all possible virtual electron-hole pairs on interacting i -th and j -th ions (see Fig.5). The sign

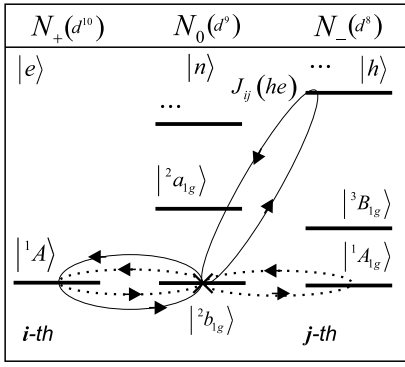


FIG. 5. Graphic representation of electron-hole pairs for interacting i -th and j -th Cu^{2+} ions. Each pair corresponds to the double exchange loop (solid or dotted lines)

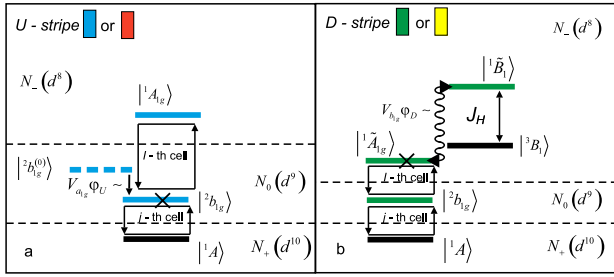


FIG. 6. Graphic scheme of energy levels of CuO_6 octahedron in different sectors N_0 and N_{\pm} configuration space in U and D stripe of the CuO_2 layer. (a) The dashed line shows the level of the hypothetical nontilted octahedron $|^1b_{1g}^{(0)}\rangle$, as well as a symmetrical a_{1g} relaxation processes. (b) The wavy line shows the JT interaction between $|^1\tilde{A}_{1g}\rangle$ and $|^1\tilde{B}_{1g}\rangle$ states in N_- sector. Loops show the virtual electron-hole pairs on interacting i -th and j -th Cu^{2+} ions.

of the $J_{ij}(h, e)$ contribution to the J_{ij}^{tot} interaction is determined by a simple rule. If the spins of an electron and a hole in a virtual pair are equal, $\hat{S}_h = \hat{S}_e$ this is the AFM contribution. If $\hat{S}_h = \hat{S}_e \pm 1$ it's FM contribution. Other terms are missing, and all electron-hole wave functions $|h\rangle$ and $|e\rangle$ in the hopping integral $t_{ij}^{hn, en} = \sum_{\lambda\lambda'} t_{ij}(\lambda\lambda') \sum_{\sigma} \gamma_{\lambda\sigma}^*(hn) \gamma_{\lambda'\sigma}(en)$ ⁴⁹⁻⁵¹ in the superexchange

$$J_{ij}^{tot} = \sum_{h,e} J_{ij}(hn, en), J_{ij}(hn, en) = \frac{2 \left(t_{ij}^{hn, en} \right)^2}{\Delta(hn, en)}, \quad (7)$$

$$\Delta(hn, en) = \varepsilon_h + \varepsilon_e - 2\varepsilon_n,$$

are calculated in the adiabatic approximation. The pairs of indices hn and en run over all possible quasiparticle excitations (n, e) and (n, h) between many-electron states $|n\rangle$ and $|e(h)\rangle$ with energies ε_n and ε_n in the sectors N_0 and N_{\pm} of configuration space in Fig.6a,b.

These quasiparticle excitations are described by non-diagonal elements $t_{ij}^{nh, ne}$. In Hubbard's model there is only one such element corresponding to the excitations between lower and upper Hubbard bands. In cuprates, the main contribution from the electron-hole pair with $|n\rangle = ^2b_{1g}$, $|h\rangle = ^1A_{1g}$ and $|e\rangle = ^1A$ has an AFM character $J_{ij}^{tot} \approx J_{ij}^{(U)}(^1A^2b_{1g}, ^1A_{1g}^2b_{1g})$ (see Fig.6a,b),⁵² where

$$J_{ij}^{(U)}(^1A^2b_{1g}, ^1A_{1g}^2b_{1g}) = \frac{2t_{ij}^2}{\Delta(^1A^2b_{1g}, ^1A_{1g}^2b_{1g})} \approx 0.15\text{eV} \quad (8)$$

where $\Delta(^1A^2b_{1g}, ^1A_{1g}^2b_{1g}) = \varepsilon_{^1A_{1g}} - 2(\varepsilon_{^2b_{1g}} - V_{a_{1g}}\alpha_U) = U_H$ and $\varepsilon_{^1A_{1g}} = 2(\varepsilon_{^2b_{1g}} - V_{a_{1g}}\alpha_U) + U_H$. However, the transverse percolation of the interaction exchange interaction $J_{i_R j_B}^{tot}$, where i_R and j_B octahedra CuO_6 are into different red(R) and blue(B) stripes at the static regular Y/R/G/B... stripe structure, is unlikely.

3.2 If there is no spontaneous θ -symmetry breaking and the JT cell state is four-fold degenerate, then the exchange interaction in the JT cell presented above is incomplete. In the novel configuration space, the states of CuO_6 octahedra with the tilting α_D angle and orientation θ_D in U stripes, and with the tilting α_U angle and orientation θ_U in D stripes are impossible. It's just that the i -th CuO_6 octahedron (the black point in Fig.7b) can simultaneously be at the U and D stripe states of any color of four R,B and G,Y possible. The novel quasiparticle excitations do not destroy the configuration space, if these quasiparticles are accompanied by changes $\delta\alpha = \alpha_D - \alpha_U$ and $\delta\theta = \theta_D - \theta_U$ shown in Fig.7b

To obtain the contributions into $J_{ij}(hn, en)$ from the electron-hole pairs with changing angles $\delta\alpha$ and $\delta\theta = \pm 45^\circ$ in the JT cell we need i -th (CuO_6 octahedron $|h_{\theta_D \alpha_D}\rangle$ and $|n_{\theta_U \alpha_U}\rangle$ states, where the indices U and D denote the stripe affiliation for the i -th octahedron

$$|h_{\theta_D \alpha_D}\rangle = |\tilde{h}\rangle |\chi_{\theta_D} \chi_{\alpha_D}\rangle; |n_{\theta_U \alpha_U}\rangle = |n\rangle |\chi_{\theta_U} \chi_{\alpha_U}\rangle \quad (9)$$

where $|\tilde{h}\rangle = |^1\tilde{A}_{1g}\rangle, |^1\tilde{B}_{1g}\rangle$ and $|n\rangle = |^2b_{1g}\rangle$. Each of R,G,B,Y colors in Fig.7b corresponds to a harmonic oscillator wave function $|\chi_{\theta}\rangle$ for a displaced 2D oscillator. These states differ by $|\chi_{\alpha_D}(Q_{\alpha} + \alpha_D)\rangle, |\chi_{\theta_D}(Q_{\theta_D})\rangle$ and $|\chi_{\alpha_U}(Q_{\alpha} + \alpha_U)\rangle, |\chi_{\theta_U}(Q_{\theta_U})\rangle$, and the matrix elements $\gamma_{\lambda\sigma}(r)$ in Eq.(8) at the i -th CuO_6 octahedron cell will be calculated on the functions $|h_{\theta_D \alpha_D}\rangle$ and $|n_{\theta_U \alpha_U}\rangle$ located at the four equivalent nuclear configurations of the JT cell corresponding to the phase θ_n (see black dot in Fig.7b).

In other words, the hole creation in the i -th CuO_6 octahedron of the $U(\theta_U)$ stripe is possible, but only if one also belongs to the $D(\theta_D)$ stripe, where $\delta\theta = \theta_D - \theta_U = \pm 45^\circ$. Thus, the matrix elements $\gamma_{\lambda\sigma}(hn)$ contain the vibronic

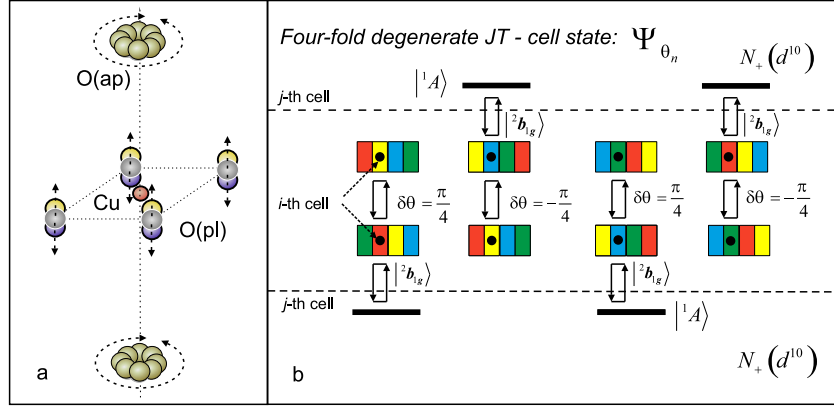


FIG. 7. (a) Graphical representation of anisotropic non-local effects in the CuO_6 octahedron located in the JT cell with fourfold degeneracy. (b) Graphical diagram of electron-hole pairs contributing to the exchange interaction when both i -th and j -th magnetic ions are in a JT cell with fourfold degeneracy. Here, the U and D stripe widths are shown the same to demonstrate the appearance of an ideal CuO_2 layer with mobile hole carriers only at the equal stripe widths

reduction factors or partial dynamical quenching:⁵³

$$J_{ij} \left({}^1\tilde{A}_{1g}, {}^1A_1 \right) = \frac{2 \left(t_{ij}^{{}^1\tilde{A}_{1g} {}^2b_{1g}, {}^1A_1 {}^2b_{1g}} \right)^2}{\Delta \left({}^1\tilde{A}_{1g} {}^2b_{1g}, {}^1A_1 {}^2b_{1g} \right)} \approx \quad (10)$$

$$\approx \frac{2u^2(\alpha_D) \cdot t_{ij}^2(x^2, x^2)}{\Delta \left({}^1\tilde{A}_{1g} {}^2b_{1g}, {}^1A_1 {}^2b_{1g} \right)} \cdot \exp \left\{ -\frac{\delta\theta^2 + \delta\alpha^2}{4} \right\}$$

where

$$t_{ij}^{{}^1\tilde{A}_{1g} {}^2b_{1g}, {}^1A_1 {}^2b_{1g}} = t_{ij}(x^2, x^2) \sum_{\sigma} \gamma_{x^2\sigma}^* \left({}^1\tilde{A}_{1g}, {}^2b_{1g} \right) \gamma_{x^2\sigma} \left({}^1A_1, {}^2b_{1g} \right) + t_{ij}(z^2, z^2) \sum_{\sigma} \gamma_{z^2\sigma}^* \left({}^1\tilde{B}_{1g}, {}^2b_{1g} \right) \gamma_{z^2\sigma} \left({}^1\tilde{B}_1, {}^2b_{1g} \right) \approx \quad (11)$$

where $\Delta \left({}^1\tilde{A}_{1g} {}^2b_{1g}, {}^1A_1 {}^2b_{1g} \right) = 2 \left[\varepsilon_{-}(\alpha_D) - \varepsilon_{{}^2b_{1g}} \right] + U_H$, and $t_{ij}(x^2, x^2) \gg t_{ij}(z^2, z^2)$. The matrix elements in Eq.(8) are equal to the following expression

$$\gamma_{x^2\sigma} \left({}^1\tilde{A}_{1g}, {}^2b_{1g} \right) = u(\alpha_D) \cdot \langle \chi_{i\theta_D} | \chi_{i\theta_U} \rangle \cdot \langle \chi_{i\alpha_D} | \chi_{i\alpha_U} \rangle \quad (12)$$

where

$$\langle \chi_{i\theta_D} | \chi_{i\theta_U} \rangle \cdot \langle \chi_{i\alpha_D} | \chi_{i\alpha_U} \rangle = \langle \chi_{i\alpha_D} (Q_{\alpha} + \alpha_D) \chi_{i\theta_D} (\theta_D) | \chi_{i\alpha_U} (Q_{\alpha} + \alpha_U) \chi_{i\theta_U} (\theta_U) \rangle \approx \exp \left\{ -(\delta\theta^2 + \delta\alpha^2)/4 \right\} \quad (13)$$

and $\delta\alpha = \alpha_D - \alpha_U \approx 5 \div 10^\circ$. Thus, at an absence of spontaneous θ -symmetry breaking, the homogeneous superexchange interaction in the hole-doped $LSCO$ cuprates is equal to

$$J_{ij}^{tot} \approx J_{ij} \left({}^1\tilde{A}_{1g} {}^2b_{1g}, {}^1A_1 {}^2b_{1g} \right) \cdot u^2(\alpha_D) \cdot \exp \left\{ -\frac{\delta\theta^2 + \delta\alpha^2}{4} \right\} \quad (14)$$

Note that, even with the at $\delta\alpha \rightarrow 0$ (weak JT effect), the result (14) does not reduce to Eq.(8). The result is independent of the choice of a i and j pair of interacting CuO_6 octahedra and the exchange J_{ij}^{tot} is homogeneous in the ideal CuO_2 layer with nonlocal effects. Indeed the neutron experiments in LCO cuprates demonstrate the thermal anisotropic motion⁵⁴ similar to the oxygen ions motion shown in Fig.7a. Similar reduction factors in the n doped $LNCO$ cuprates are impossible, since there is no JT effect in the N_+ (d^{10}) electron sector.

IV. CONCLUSIONS

The JT pseudo effect in the N_- (d^8) hole sector with a hole concentration exceeding a threshold magnitude x_c is accompanied by the charge and spin inhomogeneities due to the nonzero tilting angle $\alpha_D \approx 10 \div 14^\circ$ of CuO_6 octahedra at the orientation angle θ_D (b_{1g} -tilting mode)

in $D(\theta_D)$ stripes surrounded by the two rock salt LaO layers. $U(\theta_U)$ stripes with CuO_6 octahedra tilted by the angle $\alpha_U \approx 5^\circ$ and oriented at the angle θ_U form dielectric regions. Note our arguments in favor of the JT nature of the charge inhomogeneity is an alternative to that competition between kinetic energy and Coulomb repulsion could cause holes to segregate into strip structures.⁵⁵

The observed regular line and checkerboard stripe structures with the chromatic number $\chi = 2$ generate a novel element of symmetry in CuO_2 layer: simultaneously rotating all tilted CuO_6 octahedra by the $\delta\theta = n \cdot (45^\circ)$ angle around the c axis. Wherein we can choose the novel JT cell, during the translation of which the initial structure and the number of hole carriers and spins in the JT cell are saved. The state Ψ_{θ_n} of the JT cell is fourfold degenerate by the initial phase $\theta_n = 0, 45^\circ, 90^\circ, 135^\circ$, and all four states can be obtained by the novel symmetry operation. In particular, any CuO_6 octahedron can be located simultaneously, both in $U(\theta_U)$ and $D(\theta_D)$ stripes without a well specific orientation $\theta_D(\theta_U)$ and tilting $\alpha_D(\alpha_U)$ angles. The exchange interaction J_{ij}^{tot} will be different depending on whether spontaneous phase θ -symmetry breaking occurs or not:

(i) The spontaneous θ -symmetry breaking leads to a static spatial distribution of the $U(\theta_U)$ and $D(\theta_D)$ stripes in doped $LSCO$. In the static structure of the CuO_2 layer, the superexchange interaction has Anderson's form $J_{ij}^{(U)} = 2t^2/U_H$ for interacting ions Cu^{2+} with spin $1/2$, but is limited in space by $U(\theta_U)$ stripes with zero hole concentration $x = 0$. However, a transverse percolation of the homogeneous exchange interaction in

a static regular line Y/R/G/B and checkerboard stripe structures is unlikely.

(ii) Without spontaneous θ -symmetry breaking, a novel JT cell can be constructed in the periodic stripe nanostructure with the fourfold degenerate Ψ_{θ_n} state. The ideal CuO_2 structure with nonlocal anisotropic effects and the homogeneous superexchange are restored. The stripe boundaries, spin and charge inhomogeneities disappear. The superexchange is suppressed from its magnitude $J_{ij}^{(U)}$ (in the nondoped LCO cuprate) by the exponential factor $J_{ij}^{tot} \approx J_{ij}^{(U)} \cdot u^2(\alpha_D) \cdot \exp\{-(\delta\alpha_D^2 + \delta\theta_D^2)/4\}$ due to dynamical quenching for the CuO_6 octahedron surrounded by two LaO rock salt layers. The conclusion does not contradict the results, where the low-temperature optical pump, soft x-ray probe measurements¹³ detected the unexpected gapless nature of the charge order. Indeed, a characteristic tunneling JT splitting $\leq 10sm^{-1}$ (1meV)⁵⁶ has the observed energy scale of the transverse fluctuations observed in $LBCO$.¹³ As follows from Fig.7b, the doping dependence of superexchange manifests itself in the form of inhomogeneity only at the different stripe widths, since the CuO_6 octahedra located in the $D(U)$ stripes begin to predominate at increasing(decreasing) hole concentration x , and therefore the θ -symmetry disappears.

(iii) In n-type $LNCO$ cuprates, the JT effect in $N_+(d^{10})$ configuration sector is impossible. In contrast to p-type $LSCO$, the superexchange interaction J_{ij} in n-type $LNCO$ cuprates should not be subject to dynamical quenching, but disappear at the high electron doping.

This work was supported by Russian Science Foundation research grant RSF No.22-22-00298.

* gav@iph.krasn.ru

¹ A. Bussmann-Holder, H. Keller, and A. Bianconi, eds., *High-TC Copper Oxide Superconductors and Related Novel Materials* (Springer Series in Materials Science; Springer International Publishing AG, Vol 255, 2017).

² T. Egami, "High- tc copper oxide superconductors and related novel materials," (Springer Series in Materials Science; Springer International Publishing AG, 2017) Chap. Alex and the Origin of High-Temperature Superconductivity, pp. 35–46.

³ G. Benedek and K. Muller, *Phase Separation in Cuprate Superconductors* (World Scientific, 1993).

⁴ A. Bianconi, S. Agrestini, G. Bianconi, D. Di Castro, and N. Saini, *J. Alloys Compd.* **317**, 537 (2001).

⁵ H. Zhao, Z. Ren, B. Rachmilowitz, J. Schneeloch, R. Zhong, G. Gu, Z. Wang, and I. Zeljkovic, *Nat. Mater.* **18**, 103 (2019).

⁶ I. Maggio-Aprile, C. Berthod, N. Jenkins, Y. Fasano, A. Piriou, and O. Fischer, "Nanoscience and engineering in superconductivity. nanoscience and technolog," (Springer-Verlag Berlin Heidelberg, 2010) Chap. Scanning Tunneling Spectroscopy of High T_c Cuprates.

⁷ O. Fischer, M. Kugler, I. Maggio-Aprile, B. C., and R. C.,

Rev. Mod. Phys. **79**(1), 353 (2007).

⁸ E. da Silva Neto, P. Aynajian, A. Frano, R. Comin, E. Schierle, E. Weschke, A. Gynis, J. Wen, J. Schneeloch, Z. Xu, S. Ono, G. Gu, M. Le Tacon, and A. Yazdani, *Science* **343**, 393 (2014).

⁹ J. Ma, *Scanning Tunneling Microscopy Studies of Single Layer High-Tc Cuprate $Bi_2Sr_{2-x}La_xCuO_6+\delta$* , Ph.D. thesis, Boston College (2009).

¹⁰ A. Lanzara, N. Saini, M. Brunelli, A. Valletta, and A. Bianconi, *Journal of Superconductivity* **10**, 319 (1997).

¹¹ G. Campi, A. Bianconi, N. Poccia, G. Bianconi, L. Barba, D. Arrighetti, G. Innocenti, J. Karpinski, N. Zhigadlo, S. Kazakov, M. Burghammer, M. V. Zimmermann, M. Sprung, and A. Ricci, *Nature* **525**, 359 (2015).

¹² R. Comin and A. Damascelli, *Annu. Rev. Condens. Matter Phys.* **7**, 369–405 (2016).

¹³ M. Mitrano, S. Lee, A. Husain, L. Delacretaz, M. Zhu, G. de la Peña Munoz, S. X-L Sun, Y. IL Joe, A. Reid, S. Wandel, G. Coslovich, W. Schlotter, T. van Driel, J. Schneeloch, G. Gu, S. Hartnoll, N. Goldenfeld, and P. Abbamonte, *Sci. Adv.* **5**(8), eaax3346(1 (2019).

¹⁴ G. Campi and A. Bianconi, *Condens. Matter* **6**(4), 40 (2021).

¹⁵ J. Zaanen and O. Gunnarsson, Phys. Rev. B **40**, 7391 (1989).

¹⁶ J. M. Tranquada, B. J. Sternlieb, J. D. Axe, Y. Nakamura, and S. Uchida, Nature **375**, 561–563 (1995).

¹⁷ M. Fujita, H. Goka, K. Yamada, J. M. Tranquada, and L. P. Regnault, Phys. Rev. B **70**, 104517(1 (2004).

¹⁸ M. Hucker, M. van Zimmermann, G. D. Gu, Z. J. Xu, J. S. Wen, G. Xu, H. J. Kang, A. Zheludev, and J. M. Tranquada, Phys. Rev. B **83**, 104506(1 (2011).

¹⁹ M. Fujita, H. Hiraka, M. Matsuda, M. Matsuura, J. Tranquada, S. Wakimoto, G. Xu, and K. Yamada, J. Phys. Soc. Jpn. **81**, 011007 (2012).

²⁰ J. J. Wen, H. Huang, S. J. Lee, H. Jang, J. Knight, Y. S. Lee, M. Fujita, K. M. Suzuki, S. Asano, S. A. Kivelson, C.-C. Kao, and J.-S. Lee, Nat. Commun. **10**, 3269(1 (2019).

²¹ H. Miao, G. Fabbris, R. J. Koch, D. G. Mazzone, C. S. Nelson, R. Acevedo-Esteves, G. D. Gu, Y. Li, T. Yilmaz, K. Kaznatcheev, E. Vescovo, M. Oda, T. Kurosawa, N. Momono, T. Assefa, I. K. Robinson, E. S. Bozin, T. J. M. P. D. Johnson, and D. M. P. M, NPJ Quantum Mater. **6**, 31(1 (2021).

²² Q. Ma, K. C. Rule, Z. W. Cronkwright, M. Dragomir, G. Mitchell, E. M. Smith, S. Chi, A. I. Kolesnikov, M. B. Stone, and B. D. Gaulin, Phys. Rev. Res. **3**, 023151 (2021).

²³ P. W. Anderson, Science **235**, 1196 (1987).

²⁴ D. Scalapino, Phys. Rep. **250**, 329 (1995).

²⁵ E. Dagotto, Rev. Mod. Phys. **66**, 763 (1994).

²⁶ Y. A. Izyumov, Physics-Uspokhi **42** (3), 215 (1999).

²⁷ P. W. Anderson, Phys. Rev. **115**, 2 (1959).

²⁸ R. Coldea, S. M. Hayden, G. Aeppli, T. Perring, C. D. Frost, T. E. Mason, S.-W. Cheong, and Z. Fisk, Phys. Rev. Lett. **86**, 5377 (2001).

²⁹ G. Bascaran, Z. Zou, and A. P. W, Solid State Commun. **63**, 973 (1987).

³⁰ C. Gros, R. Joynt, and T. M. Rice, Phys. Rev. B **36**, 381 (1987).

³¹ G. Kotliar and J. Liu, Phys. Rev. B **38**, 5142 (1988).

³² Y. Suzumura, Y. Hasegawa, and H. Fukuyama, J. Phys. Soc. Jpn. **57**, 2768 (1988).

³³ P. Prelovsek and A. Ramsak, Phys. Rev. B **72**, 012510(1 (2005).

³⁴ N. M. Plakida, L. Anton, S. Adam, and G. Adam, JETP **97**(2), 331 (2003).

³⁵ J. Rossat-Mignod, L. P. Regnault, C. Vettier, P. Bourges, P. Burlet, J. Bossy, J. Y. Henry, and G. Lapertot, Physica C: Superconductivity **185-189**, 86 (1991).

³⁶ H. F. Fong, P. Bourges, Y. Sidis, L. P. Regnault, J. Bossy, A. Ivanov, D. L. Milius, I. A. Aksay, and B. Keimer, Phys. Rev. B **61**, 14773 (2000).

³⁷ P. Dai, H. A. Mook, R. D. Hunt, and F. Do?an, Phys. Rev. B **63**, 054525(1 (2001).

³⁸ V. A. Gavrichkov, Y. Shan'ko, N. G. Zamkova, and A. Bianconi, J. Phys. Chem. Lett **10**, 1840 (2019).

³⁹ A. Bianconi, N. L. Saini, A. Lanzara, M. Missori, and T. Rossetti, Phys Rev Lett. **76**, 3412 (1996).

⁴⁰ A. M. Glazer, Phase Transitions **84**, 405 (2011).

⁴¹ R. B. Woodward and R. Hoffmann, *The Conservation of Orbital Symmetry* (Verlag Chemie GmbH, Academic Press Inc., 1971).

⁴² E. Kano, D. G. Kvashnin, S. Sakai, L. A. Chernozatonskii, P. B. Sorokin, A. Hashimoto, and T. M. Nanoscale **9**, 3980 (2017).

⁴³ D. G. Kvashnin, A. G. Kvashnin, E. Kano, A. Hashimoto, M. Takeguchi, H. Naramoto, S. Sakai, and P. B. Sorokin, J. Phys. Chem. C **123**(28), 17459 (2019).

⁴⁴ J. Rodriguez-Carvajal, M. T. Fernandez-Diaz, and J. L. Martinez, J. Phys.: Condens. Matter **3**, 3215 (1991).

⁴⁵ Zhang and T. M. Rice, Phys. Rev. B **37**, 3759 (1988).

⁴⁶ G. I. Bersuker, N. N. Gorinchoy, V. Z. Polinger, and A. O. Solonenko, Supercond.: Phys., Chem., Eng. **5**, 1003 (1992).

⁴⁷ J. Hubbard, Proc. Roy. Soc. **84**, 455 (1964).

⁴⁸ V. A. Gavrichkov and S. A. Gavrichkov, Phys.Lett. A **145**(6-7), 353 (1990).

⁴⁹ V. A. Gavrichkov, S. I. Polukeev, and S. G. Ovchinnikov, Phys. Rev. B **101**, 094409(1 (2020).

⁵⁰ V. A. Gavrichkov, S. I. Polukeev, and S. G. Ovchinnikov, Phys. Rev.B **95**, 144424(1 (2017).

⁵¹ R. Mikhaylovskiy, T. Huisman, V. Gavrichkov, S. I. Polukeev, S. Ovchinnikov, D. Afanasiev, R. Pisarev, T. Rasing, and A. Kimel, Phys. Rev. Lett. **125**, 157201(1 (2020).

⁵² V. A. Gavrichkov, Z. V. Pchelkina, I. A. Nekrasov, and O. S. G, Int. J. Mod. Phys. B **30**, 1650180(1 (2016).

⁵³ F. S. Ham, Phys. Rev. **138**, A1727 (1965).

⁵⁴ P. S. Hafliger, S. Gerber, R. Pramod, V. I. Schnells, B. dalla Piazza, R. Chati, V. Pomjakushin, and K. Conder, Phys Rev B **89**, 085113(1 (2014).

⁵⁵ M. Imada, Journal of the Physical Society of Japan **90**, 111009(1 (2021).

⁵⁶ I. B. Bersuker, *Electronic Structure and Properties of Transition Metal Compounds: Introduction to the Theory*, edited by 2nd Edition (John Wiley & Sons: New-York, 2010).